JOURNAL OF SPACECRAFT AND ROCKETS
Vol. 34, No. 3, May–June 1997

Heliospheric Boundary Exploration Using Ion Propulsion Spacecraft

Craig A. Kluever*
University of Missouri–Columbia/Kansas City, Kansas City, Missouri 64110-2499

A new deep-space mission to the heliospheric boundary is analyzed for spacecraft utilizing low-thrust ion engines. The mission design is performed by optimizing a combination of trajectory variables and propulsion system parameters such that the total trip time to the heliospheric boundary is minimized. Spacecraft utilizing both solar electric propulsion and nuclear electric propulsion are considered. Optimal mission designs are presented for a wide range of launch vehicle options. In addition, a sensitivity analysis of the assumed electric propulsion technology level and gravity-assist flyby conditions is performed. Although electric propulsion is typically associated with payload fraction enhancement, this analysis demonstrates that the use of low-thrust spacecraft results in relatively short trip times for high-energy deep-space missions. Furthermore, it is shown that the performance of both electric-propulsion spacecraft trajectories compare favorably and in many cases show improvement over missions utilizing all-chemical propulsion systems.

Nomenclature

b = propellant dependent coefficient
C_3 = launch energy, km^2/s^2
c = engine exhaust velocity, km/s
d = propellant dependent coefficient, km/s
$\boldsymbol{f}$ = state differential equation vector
g = sea-level gravitational acceleration, m/s^2
$\boldsymbol{h}$ = initial boundary condition vector
I_{sp} = specific impulse, s
J = performance index, years
K_t = tankage fraction
m = spacecraft mass, kg
m_{net} = net mass of spacecraft, kg
m_{pp} = mass of power and propulsion system, kg
m_{prop} = propellant mass, kg
m_{tank} = mass of tank and propellant feed system, kg
$\boldsymbol{N}$ = interior-point state constraint vector
P = input power, kW
$\boldsymbol{r}$ = spacecraft heliocentric position vector, AU
r_{FB} = planetary flyby radius, planet radii
$\boldsymbol{r}_P$ = target planet heliocentric position vector, AU
T = thrust magnitude, N
t_f = arrival date
t_i = planetary flyby date
t_0 = launch date
$\boldsymbol{u}$ = thrust direction unit vector
$\boldsymbol{x}$ = state vector
α = specific mass of the power and propulsion system, kg/kW
β = propellant mass flow rate, kg/s
ΔV_{GA} = velocity increment from gravity assist, km/s
η = thruster efficiency
θ = longitude angle, deg
$\boldsymbol{\psi}$ = terminal state constraint vector

Subscripts

f = final (arrival)
i = planetary flyby
0 = initial (launch)
200 = at heliospheric boundary, where r is 200 AU

Received Nov. 5, 1996; revision received March 14, 1997; accepted for publication March 14, 1997.

*Assistant Professor, Mechanical and Aerospace Engineering Department. Member AIAA.

Introduction

THE first new millennium interplanetary space mission proposed by NASA will use electric propulsion (EP) as the primary mode of propulsion.[1] For this particular mission, the spacecraft will use solar electric propulsion (SEP) and a 30-cm ion engine with xenon as the propellant. In addition, a fast Pluto flyby mission using near-term SEP technology has been recently investigated.[2] Other EP mission studies include both crewed and uncrewed lunar and Mars missions using nuclear electric propulsion (NEP).[3–6] The payload advantages of using low-thrust EP in comparison to conventional chemical propulsion have been demonstrated by numerous authors for a variety of space missions.[7,8]

A particular deep-space mission of recent interest is the exploration of the heliospheric boundary of our solar system. Mewaldt et al.[9] outlined a mission to send a small spacecraft to the heliosphere via chemical propulsion. The heliospheric boundary consists of the interaction between the solar wind and interstellar plasma and the upper limit of this boundary is estimated to be at about 200 AU (Ref. 9). Very little is known about the structure of the heliosphere, and the primary objective of such a mission would be in situ measurements of the particles, plasma, and fields at the heliospheric boundary.[9] In addition, a spacecraft enroute to the heliospheric boundary may be able to encounter Neptune or Pluto and, therefore, enhance the scientific return.

This paper presents several mission designs for heliospheric boundary exploration using spacecraft with low-thrust ion engines as the primary mode of propulsion. The mission design goal is to transfer a 200-kg spacecraft to the heliospheric boundary in minimum time. The mission design is a combined trajectory and propulsion system optimization problem. Trajectory design variables include launch date, launch energy, burn and coast arc switch times, thrust steering direction, and planetary flyby conditions. Propulsion system design parameters include input power and specific impulse. Both SEP and NEP spacecraft are considered, and a wide range of launch vehicle options are investigated. Numerical results are presented, and comparisons with the all-chemical heliospheric missions from Ref. 9 are made.

Mission Definition

As mentioned and in accordance with Ref. 9, the objective of the mission is to transfer a spacecraft with a net mass of 200 kg to the heliospheric boundary at 200 AU within a reasonable total mission lifetime. To minimize the total trip time, the general direction of the trajectory should be toward the nose of the heliosphere, which is the direction of the velocity vector of the solar system. In the heliocentric-ecliptic coordinate frame, this incoming direction of the interstellar plasma corresponds to 254.5° longitude and 7.5°

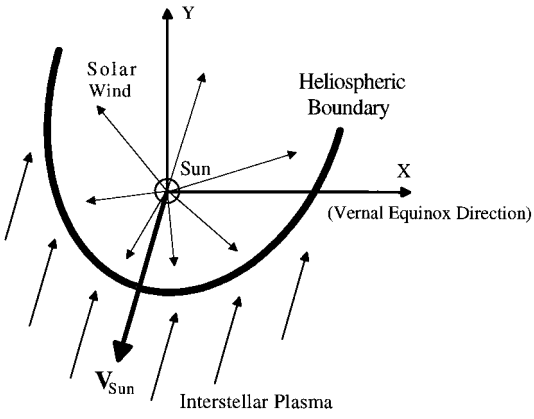

Fig. 1 Orientation of the heliospheric boundary.

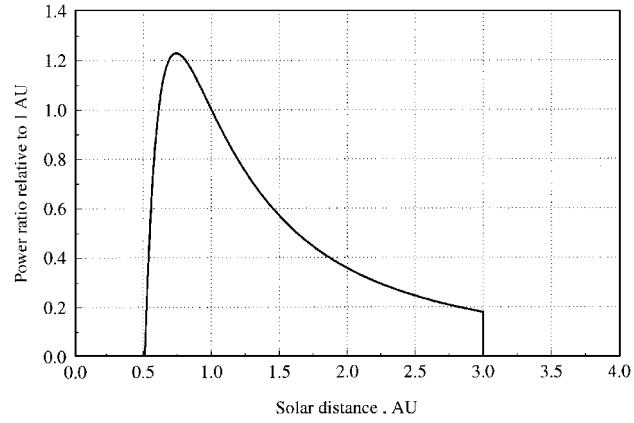

Fig. 2 Solar array power ratio relative to 1 AU.

latitude. Figure 1 shows a schematic of the orientation of the heliosphere. Therefore, the goal of the trajectory and propulsion system optimization problem is to obtain the minimum-time transfer to the heliospheric boundary just defined.

Because the mission definition calls for a net mass of 200 kg, the net spacecraft mass m_{net} is defined as

$$m_{\text{net}} = m_0 - m_{\text{prop}} - m_{\text{tank}} - m_{\text{pp}} \tag{1}$$

The spacecraft's net mass represents the usable mass for payload plus the basic spacecraft structural mass. The initial mass of the spacecraft m_0 on injection into heliocentric space is computed from launch vehicle performance curves with hyperbolic excess energy (C_3) as the independent variable. Tank mass m_{tank} is the product of the tankage fraction K_t and the total EP propellant mass m_{prop}, and the mass of the EP power and propulsion system m_{pp} is the product of specific mass α and input power P. The vehicle parameters K_t and α represent the assumed technology level for EP spacecraft, and their respective values are presented in the following sections.

Trajectory and Propulsion System Optimization

SEP Model

The SEP system is modeled with thrust magnitude T dependent on input power P, thruster efficiency η, and specific impulse I_{sp}:

$$T = 2\eta P/c \tag{2}$$

where $c = gI_{\text{sp}}$ is the engine exhaust velocity. Propellant mass flow rate β is related to thrust as follows:

$$\beta = T/c \tag{3}$$

It is assumed that xenon is utilized as the propellant for the EP system and, therefore, thruster efficiency η is determined by the following relation using I_{sp} and propellant-dependent coefficients derived from theoretical models and experimental data[4]:

$$\eta = \frac{bc^2}{c^2 + d^2} \tag{4}$$

where $b = 0.81$ and $d = 13.5$ km/s. Specific impulse is bounded by the following limits, which are typical for EP systems using xenon[4]:

$$200 \le I_{\text{sp}} \le 7000\,\text{s} \tag{5}$$

It is assumed that I_{sp} is constant over the entire mission, which implies a fixed engine operating point with no throttling.

For SEP spacecraft, power P from the solar arrays diminishes with distance from the sun. The power ratio relative to available power at 1 AU is modeled by the performance curve presented in Fig. 2 for a solar array with silicon cells. The power is nearly proportional to the inverse-square distance from the sun and is considered to be zero for distances greater than 3 AU and for distances less than 0.5 AU due to extreme thermal conditions. Specific mass α is fixed at 20 kg/kW, which represents near-term SEP technology,[10] and tankage fraction K_t is fixed at 10% (Ref. 11).

NEP Model

The basic system modeling for an NEP spacecraft is essentially the same as the SEP spacecraft model with the exception that thruster input power P is constant and does not change with distance from the sun. It is assumed that P does not degrade over time. Because the NEP system is assumed to utilize ion thrusters and xenon as the propellant, the basic relations for thrust, mass flow rate, efficiency, and I_{sp} range are identical to Eqs. (2–5).

To utilize the current class of launch vehicles, the nuclear reactor must be in the kilowatt range instead of the megawatt range. In Ref. 12, a derivative of the Topaz 2 reactor is proposed for deep-space interplanetary missions. The improved Stirling-cycle Topaz reactor is estimated to have a total mass of 1405 kg and produce 40 kW of power.[12] Therefore, the specific mass for this proposed nuclear power system is approximately 35 kg/kW. In Ref. 5, the specific mass for an ion propulsion system (thrusters plus power processors) using a nuclear power source is conservatively estimated at 6 kg/kW. Therefore, the specific mass α for the power and propulsion system for a kilowatt-range NEP system is estimated at 41 kg/kW. Because the specific mass typically decreases with increasing reactor size (the so-called economy of scale for NEP power systems), a lower limit for power output of the Topaz-derived system is set at 30 kW. In other words, the estimated α of 41 kg/kW is assumed to be applicable only for power output levels above 30 kW. The tankage fraction K_t remains fixed at 10% for the NEP system.

Problem Statement

The optimization problem is presented in this section. The problem statement for the heliosphere trajectory and propulsion system optimization problem is as follows.

Find the initial launch data t_0, the launch energy C_3, the durations of the multiple powered arcs, the thrust direction unit vector $\boldsymbol{u}(t)$ for the powered arcs, the changes in true longitude for the coasting arcs, the planetary flyby conditions, the input power P_0 at 1 AU, the specific impulse I_{sp}, and the final arrival date t_f, which minimize

$$J = t_f - t_0 \tag{6}$$

subject to the equations of motion in an inverse-square gravity field

$$\dot{\boldsymbol{x}}(t) = \boldsymbol{f}[t, \boldsymbol{x}(t), \boldsymbol{u}(t)] \tag{7}$$

with the initial boundary conditions

$$\boldsymbol{x}(t_0) = \boldsymbol{h}(t_0, C_3) = \boldsymbol{x}_0 \tag{8}$$

the interior-point state constraints

$$\boldsymbol{N}[\boldsymbol{x}(t_i), t_i] = \boldsymbol{r}(t_i) - \boldsymbol{r}_P(t_i) = \begin{pmatrix} 0 \\ 0 \\ 0 \end{pmatrix} \tag{9}$$

the terminal state constraints

$$\psi[\boldsymbol{x}(t_f), t_f] = \boldsymbol{r}(t_f) - \boldsymbol{r}_{200} = \begin{pmatrix} 0 \\ 0 \\ 0 \end{pmatrix} \tag{10}$$

the inequality constraints [Eq. (5)], and

$$m_{\text{net}} \geq 200\,\text{kg} \tag{11}$$

In the preceding problem formulation, the spacecraft's state is denoted by the seven-element vector $\boldsymbol{x}(t)$, where the first six elements are the spacecraft's orbital elements and the seventh element is spacecraft mass. Because the goal is to minimize the total trip time, the performance index J is the difference in final arrival date and initial departure date. The equations of motion [Eq. (7)] are with respect to a sun-centered, inverse-square gravity field and are expressed in terms of a modified equinoctial orbital element set[13] in order to allow for both elliptical and hyperbolic heliocentric trajectories. The detailed set of dynamical equations of motion for a powered spacecraft is presented in Ref. 13. The initial boundary conditions [Eq. (8)] are computed by an accurate solar system ephemeris with the Julian date of exit from the Earth's sphere of influence and launch energy C_3 as the input variables. Equation (9) represents interior-point state constraints, which require matching between the spacecraft and target planet position vectors for a planetary gravity assist. The gravity assist is modeled as an impulsive velocity change, and the details are presented in Ref. 13. The terminal state constraints [Eq. (10)] require that the final spacecraft position vector $\boldsymbol{r}(t_f)$ match the position vector of the heliospheric boundary nose at 200 AU, $\boldsymbol{r}_{200} = [-52.9904, -191.0773, 26.1052]^T$ AU, which corresponds to a latitude and longitude of 7.5° and 254.5°, respectively.

Solution Method

Because the trajectory and propulsion system optimization problem involves a mix of discrete control parameters (launch and arrival dates, powered arc durations, planetary flyby conditions, input power, I_{sp}) and continuous control functions [thrust direction unit vector $\boldsymbol{u}(t)$ during the powered arcs], the problem just outlined is solved using a direct optimization method. More specifically, the optimal control problem is replaced by a nonlinear programming (NLP) problem, which in turn is solved by using sequential quadratic programming (SQP), a constrained parameter optimization method.[14] The SQP code used computes the required partial derivatives with first-order forward differences.[15] The thrust direction control functions $\boldsymbol{u}(t)$ are parameterized by linear interpolation through a discrete set of control nodes. Therefore, the control nodes (for each powered arc) are SQP design variables. Six nodes for each thrust direction component per powered arc were deemed sufficient for acceptable trajectory control. Trajectory generation is accomplished by numerically integrating the powered equations of motion [Eq. (7)] with a standard fourth-order, fixed-step, Runge–Kutta routine. Acceptable numerical accuracy for the trajectory was achieved with 200 integration steps per powered arc. Coast arcs are computed by using analytical methods from two-body orbital mechanics. Planetary flybys for gravity assists are treated as impulsive velocity changes and are computed via two-body analytical methods by specifying the flyby orbit plane orientation and flyby periapsis radius (see Ref. 13 for more details). Therefore, these two parameters (per gravity assist) are also included as SQP design variables. Because the optimal control problem is solved as a NLP problem, the number of powered and coast arcs, as well as the number and sequence of planetary flybys, must be specified in advance.

Finally, the terminal state constraints [Eq. (10)], which maintain arrival at the heliospheric boundary nose, are enforced through three SQP equality constraints. In addition, the interior-point state constraints [Eq. (9)] are also enforced through a set of three SQP equality constraints per flyby. The inequality constraints on the I_{sp} range as indicated by Eq. (5) are enforced through upper and lower box constraints on the appropriate SQP design variable, and the payload constraint [Eq. (11)] is enforced by an SQP inequality constraint.

Numerical Results for SEP Spacecraft

There exists a very wide range of trajectory options for the minimum-time transfer to the heliosphere boundary. For example, the launch vehicle, number of powered and coasting arcs, and number and sequence of planetary gravity assists must be specified in advance for use of the direct optimization method. For this reason, the minimum-time transfer problem is initially solved for the simplest trajectory cases, that is, cases that do not involve planetary gravity assists. By solving these simple problems, one can obtain a feel for other trajectory options such as launch vehicle selection and number of powered and coasting arcs.

Trajectories Without Gravity Assists

Four different existing launch vehicles are investigated: Med-Lite, Delta II 7925, Atlas IIAS/Star 48B, and Titan IV/Centaur. The last three are the launch vehicles used in Ref. 9 and are selected so that a direct comparison can be made between the results presented here and the trajectory results using conventional chemical propulsion systems.

The convergence properties of this numerical problem were found to be improved by first solving a maximum-energy problem without constraints on the final trajectory direction. For the maximum-energy problem, it is possible to use simple initial guesses for the design variables [such as grouping the burns at perihelion and setting the thrust direction $\boldsymbol{u}(t)$ along the local horizontal direction]. The maximum-energy problems identify trajectories that achieve solar-system escape conditions, and the corresponding solutions are then utilized as the initial guesses for the minimum-time heliopause transfer problem. The final trajectory direction constraints are satisfied during the numerical optimization process by adjusting the launch date, which essentially rotates the entire trajectory in heliocentric space.

A variety of minimum-time missions are obtained for a range of engine sequence schemes, and the results are shown in Table 1. Initially, the one-burn solution is obtained for each launch vehicle followed by the two-burn solution, three-burn solution, and so on. All of the optimal missions resulted in a net mass at the lower limit of 200 kg. The optimal launch year is not presented in Table 1 because the optimal mission opportunities will repeat annually. The best trajectory options without gravity assists exhibit a range of trip times from 46.2 (Med-Lite) to 29.4 (Titan) years. In Ref. 9, all orbit transfers using chemical propulsion required several planetary gravity assists; the fastest transfers ranged from 34.1 (Delta) to 21.8 (Titan) years. These gravity-assisted transfers using chemical propulsion will be described in further detail in the next section.

As indicated in Table 1, it is not possible to achieve escape conditions with the Med-Lite and a single SEP-powered arc. Furthermore, the total trip time decreases as the number of burn arcs is increased until an upper limit for the number of burns is reached. For the Med-Lite launch vehicle, the fastest transfer to the heliosphere requires

Table 1 Minimum-time missions to the heliospheric boundary for SEP spacecraft without gravity assists

Launch vehicle	Number of powered arcs	Launch date	Trip time, years	C_3, km^2/s^2	m_0, kg	P_0, kW	I_{sp}, s
Med-Lite	2	Nov. 22	47.3	1.51	661.5	9.4	4818.6
Med-Lite	3	Jan. 28	46.2	0.60	673.7	8.9	5012.6
Delta	1	Aug. 15	63.7	2.23	1272.9	22.2	3288.8
Delta	2	Jan. 8	35.8	2.78	1259.5	18.9	3982.9
Atlas	1	Dec. 23	46.7	61.26	957.7	19.3	2608.6
Atlas	2	Feb. 9	32.1	6.12	2280.0	34.2	3564.4
Titan	1	Jan. 2	37.1	85.43	1834.8	41.3	2437.8
Titan	2	March 14	29.4	17.24	6613.2	98.3	3208.2

Table 2 Optimal trajectory and SEP parameters for minimum-time transfers with a Jupiter gravity assist

Launch vehicle	Number of powered arcs	Launch date	Trip time, years	C_3, km^2/s^2	P_0, kW	I_{sp}, s	ΔV_{GA}, km/s
Med-Lite	3	Dec. 24, 2009	37.1	0.98	9.23	4705.5	17.2
Med-Lite	2	Nov. 1, 2001	35.1	1.63	9.26	4780.4	17.7
Delta	2	Dec. 20, 2001	30.4	3.29	18.84	3964.5	16.1
Atlas	2	Jan. 17, 2003	27.9	7.86	34.82	3477.7	15.4
Titan	2	March 2, 2003	26.4	17.92	96.87	3220.6	14.8

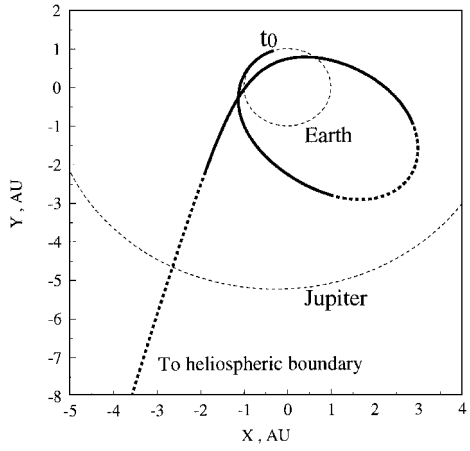

Fig. 3 Minimum-time SEP transfer: Delta without gravity assists; ——, burn and - - - -, coast.

46.2 years and involves three burns grouped near perihelion. An attempt to obtain a four-burn solution results in a trip time greater than 46.2 years, and subsequently the direct method eliminates the fourth burn arc during the optimization process. The upper limit on number of burns is two for the three larger launch vehicles, as shown in Table 1. Increasing the number of perihelion burns will decrease the propellant required for a given orbit transfer; however, the heliosphere boundary mission is a minimum-time problem and not a minimum-fuel problem. Therefore, including additional burn arcs results in additional revolutions about the sun, which increases the total trip time.

Table 1 also shows the optimal trajectory and EP system parameters for the orbit transfers for each launch vehicle. The EP power and C_3 both increase and I_{sp} decreases as the launch capability is increased. Therefore, the thrust magnitude of the SEP system is increased in order to minimize the transfer time as larger launch vehicles are employed. All of the minimum-time transfers exhibit perihelion burns near a radial distance of about 0.7 AU so that the solar array performance (as depicted by Fig. 2) is maximized. Furthermore, the final burn switching points are at a radial distance of 3 AU, which corresponds to the maximum radial distance for solar array output. Figure 3 shows the heliocentric trajectory and the two perihelion burns for the Delta launch vehicle. In this case, the trajectory achieves solar-system escape conditions during the second burn just prior to perihelion passage.

Trajectories with Gravity Assists

A variety of planetary gravity assist options are explored for the range of launch vehicles. A good guess for the optimal number of burn arcs for each launch vehicle is determined from the solutions in the preceding section.

The strategy employed here is to obtain optimal missions for the simplest gravity assist scenario possible and, subsequently, solve more difficult problems with increasingly complex gravity assist maneuvers. Therefore, the initial optimal trajectories involve a single Jupiter gravity assist after all SEP powered arcs and escape conditions have been achieved. This problem is readily solved by employing an initial guess for the optimization routine based on the previous minimum-time orbit transfers without gravity assists. Furthermore, the launch date is adjusted until the escape trajectories from the previous solutions pass near Jupiter. Two additional trajectory design variables are included in this problem: orientation of the planetary flyby plane and periapsis radius of the flyby. The lower limit of the periapsis radius is set at five Jupiter radii in accordance with gravity assist analyses.[16]

Table 3 Optimal trajectory and SEP parameters for minimum-time transfers with Earth–Jupiter gravity assists[a]

Launch vehicle	Launch date	Trip time, years	C_3, km^2/s^2	P_0, kW	I_{sp}, s	Total ΔV_{GA}, km/s	$\theta(t_f)$, deg
Med-Lite	Nov. 26, 2002	31.8	2.22	9.36	4469.9	21.5	281.0
Delta	Dec. 25, 2002	28.4	4.21	19.40	3708.3	19.5	271.7
Atlas	Jan. 12, 2003	26.7	9.52	35.66	3351.7	18.6	267.5
Titan	Jan. 31, 2003	24.8	22.43	98.90	3103.4	18.0	235.3

[a]All solutions have two perihelion powered arcs.

Table 2 presents the optimal trajectory and SEP system parameters for minimum-time transfers with a Jupiter gravity assist for the four launch vehicle options. The gravity-assisted trajectories show significant reductions in total mission time over the trajectories without gravity assists, and these mission-time reductions are more dramatic for the smaller launch vehicles. The respective trip-time reductions from using the Jupiter flyby are 11.1 (Med-Lite), 5.4 (Delta), 4.2 (Atlas), and 3.0 (Titan) years. As expected, the optimal perijove radius for the gravity assist is five Jupiter radii for all cases so that the maximum ΔV_{GA} is achieved. The magnitude of the gravity assist is shown in Table 2 and ranges from 14.8 to 17.7 km/s. The two-burn solutions for the smaller launch vehicles (Med-Lite and Delta) exhibit launch dates in late 2001, and the two-burn solutions for the larger launch vehicles (Atlas and Titan) show launch dates in early 2003. The Med-Lite and Delta trajectories require an additional year to reach Jupiter's orbit compared to the Atlas and Titan trajectories.

Initially, the minimum-time transfer with the Med-Lite was found with three perihelion burns, and the result is a trip time of 37.1 years with a launch date in late 2009. The launch date for all cases is constrained to be greater than 1999, which is a reasonable time frame for SEP technology. The three-perihelion-burn case requires an extra orbit about the sun, which adds 3.8 years to the time required to reach Jupiter's orbit as compared to the two-burn case. Therefore, to flyby Jupiter, the three-burn trajectory must depart Earth's orbit 3.8 years earlier than the two-burn case (which is unacceptable because the two-burn launch date is late 2001) or delay the launch date about 8 years because Jupiter's period is 11.86 years. Recall that for the Med-Lite trajectories without gravity assists, the three-burn case only slightly reduced the trip time to the heliospheric boundary compared to the two-burn case. Furthermore, the energy of the ballistic trajectory at Jupiter's orbit is only slightly greater for the three-burn case as compared to the two-burn case. Therefore, when a Jupiter gravity assist is included, the total mission time is substantially reduced by utilizing a two-burn trajectory, which reaches Jupiter's orbit over three years sooner than the three-burn case.

Next, a powered Earth gravity assist is included during the final perihelion burn along with the coasting Jupiter gravity assist. The lower limit of the perigee flyby altitude is set at 350 km. Table 3 shows the mission and SEP optimization results for the four launch vehicles. All four cases utilized a two-burn trajectory, and all total trip times were reduced with the largest reduction at 3.3 years (Med-Lite) and the smallest at 1.2 years (Atlas). Figure 4 shows the heliocentric trajectory for the SEP spacecraft using the Delta launch vehicle. Again, the trajectory achieves escape conditions during the second burn prior to the Earth flyby. The additional gravity assist results in an increase in C_3 and P for all four launch vehicles.

Table 4 Minimum-time transfers using chemical propulsion (from Ref. 9)

Launch vehicle	Gravity assist sequence	Trip time (one-stage), years	Trip time (two-stage), years
Delta	VEEJS	——	34.1
Atlas	VEEJS	27.7	25.4
Titan	EJS	24.5	21.8

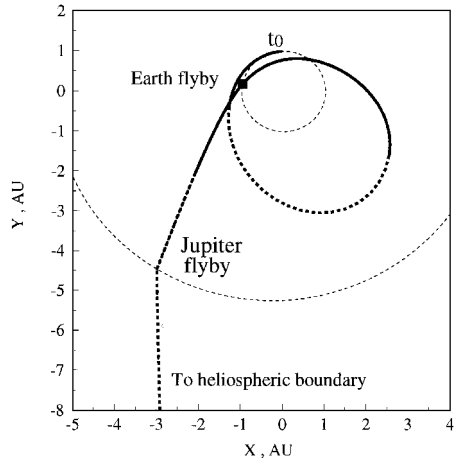

Fig. 4 Minimum-time SEP transfer: Delta with EJ gravity assists; ——, burn and - - - -, coast.

Note that the Earth–Jupiter (EJ) trajectory solutions presented in Table 3 do not satisfy the final longitude constraint of $\theta(t_f) = 254.5$ deg. For these complex trajectories with multiple perihelion burns and two planetary flybys, the final longitude constraint was relaxed because the strict enforcement of the $\theta(t_f)$ constraint added three to six years to the respective trip times. The final longitude angles in Table 3 show deviations from the desired $\theta(t_f)$ ranging from −26.5 to 19.2 deg. It is not clear from Ref. 9 whether an exact final longitude angle is necessary (or enforced in the subsequent solutions) because formal boundary conditions are not presented. Furthermore, Ref. 9 states, "the general direction of the trajectory should be toward the nose of the heliosphere, which corresponds to the ram direction of the inflowing interstellar gas." Because the trajectories presented in Table 3 are in the general direction of $\theta(t_f) = 254.5$ deg, the final longitude constraint is relaxed in favor of substantially reducing the trip time. Note that when the Jupiter gravity-assisted trajectories (Table 2) are recomputed with the final longitude constraint relaxed, the resulting trip times are only slightly reduced. In particular, the trip time reduction ranges from a minimum of 0.8 days (Med-Lite) to a maximum of 95.5 days (Titan). The worst final longitude angle for these relaxed cases is $\theta(t_f) = 239.5$ deg (Titan).

For comparison purposes, the best minimum-time transfers using chemical propulsion from Ref. 9 are presented in Table 4. These trajectories employ multiple flyby sequences including Venus–Earth–Earth–Jupiter gravity assists with a powered solar flyby (VEEJS) and Earth–Jupiter–solar flyby (EJS). Both single-stage ($I_{sp} = 308$ s) and two-stage ($I_{sp} = 290$ s) chemical propulsion systems are utilized in the analysis in Ref. 9. As indicated by comparing Tables 3 and 4, the best SEP trajectory using a Delta exhibits a trip time 5.7 years shorter than the best chemical propulsion trajectory with the same launch vehicle. In addition, the best SEP trajectory with a Med-Lite has a trip time 2.3 years shorter than the best chemical propulsion trajectory using a Delta. Furthermore, the trip time differences between the SEP and single-stage chemical systems using the Atlas and Titan are within one year.

An initial Venus gravity assist and multiple Earth gravity assists were attempted with the SEP trajectories because this strategy seems optimal for many of the chemical propulsion trajectories. In all flyby cases (VEJ, VEEJ, or EEJ), the SEP trajectories showed poorer performance than the EJ trajectories presented in Table 3. A potentially attractive gravity assist option is a double Jupiter flyby; this option is not investigated here and is reserved for future work.

Trajectories with Earth-Escape Spirals

In this section, the hyperbolic Earth-escape phase via the upper stage chemical boost from the respective launch vehicle is replaced by an SEP-powered Earth-escape spiral trajectory from circular Earth orbit. Because long-term exposure to the Van Allen radiation belts can cause substantial performance degradation to the solar arrays, the initial circular high Earth orbit (HEO) is above the radiation belts with an altitude of 51,024 km. Again, the initial spacecraft mass in HEO is determined by the respective launch vehicle performance curves. The SEP spiral time from HEO to Earth-escape conditions ($C_3 = 0$) is computed by an analytical expression developed by Perkins[17] for universal low-thrust trajectory solutions. These universal solutions can be scaled by specifying the initial circular orbit radius, initial thrust acceleration, and gravitational parameter of the attracting body. The minimum-time transfers to the heliosphere (using an EJ gravity assist) for the four launch vehicles are presented in Table 5. It can be seen that the trajectories utilizing an SEP-powered Earth-escape spiral show very little difference in trip time when compared to the trajectories using a chemically boosted hyperbolic escape trajectory. The lack of enhanced performance from the addition of the escape spiral can most likely be attributed to the relatively short spiral escape time to $C_3 = 0$. Because the spiral escape is short (due to the high-energy HEO), the advantages of the SEP system are diminished. In the case of the Titan, the increase in P (due to including the escape spiral) does not offset the high launch energy capability, and the total trip time is actually increased by 0.7 years when the escape spiral is implemented.

Sensitivity Analysis of SEP and Gravity Assist Parameters

The sensitivity of the performance index J (total trip time) to changes in SEP technology parameters (α and K_t) and a gravity assist parameter (Jupiter flyby radius r_{FB}) was computed by simple finite difference methods. The goal is to estimate the sensitivity $\partial J/\partial X$, where X is the independent parameter of interest (α, K_t, or r_{FB}). The respective sensitivities were computed by individually perturbing the parameters by 5% from their fixed values and recomputing the minimum-time transfers. Recall that the nominal values for these parameters are $\alpha = 20$ kg/kW, $K_t = 10\%$, and $r_{FB} = 5\,R_{Jov.}$ The two-burn, EJ gravity-assisted, minimum-time transfers from Table 3 were utilized as the baseline trajectories for the sensitivity analysis. Because the Jupiter gravity assist provides the largest ΔV_{GA} contribution, only that flyby radius was perturbed for the analysis.

Table 6 presents the three performance sensitivities for the four launch vehicles. In general, the performance of the smaller launch vehicles (Med-Lite and Delta) is more sensitive to changes in α and r_{FB} and less sensitive to changes in K_t than the performance

Table 5 Optimal trajectory and SEP parameters[a] for minimum-time transfers using an Earth-escape spiral to $C_3 = 0$

Launch vehicle	Launch date	Trip time, years	Escape time, days	P_0, kW	I_{sp}, s	Total ΔV_{GA}, km/s	$\theta(t_f)$, deg
Med-Lite	Sept. 8, 2002	31.3	51.8	11.15	4592.2	21.4	251.7
Delta	Oct. 8, 2002	28.1	43.6	22.54	3945.1	19.8	243.1
Atlas	Oct. 20, 2002	26.7	41.0	42.15	3657.8	18.9	239.3
Titan	Oct. 29, 2002	25.5	39.9	140.1	3394.9	18.3	236.3

[a]All solutions employ EJ gravity assists and have two perihelion-powered arcs.

Table 6 Performance sensitivity to SEP and gravity assist parameters[a]

Launch vehicle	$\partial J/\partial\alpha$, years-kW/kg	$\partial J/\partial K_t$, years/%	$\partial J/\partial r_{FB}$, years/$R_{Jov}$
Med-Lite	0.36	0.09	0.70
Delta	0.32	0.10	0.49
Atlas	0.31	0.10	0.41
Titan	0.31	0.12	0.36

[a]All trajectories employ EJ gravity assists.

of the larger vehicles. However, the performance sensitivity due to the SEP parameters α and K_t exhibits a slight variation across the launch vehicle spectrum. In contrast, the performance sensitivity due to the Jupiter flyby radius nearly doubles between the Med-Lite and Titan vehicles. Using this simple linear analysis, increasing α from 20 to 35 kg/kW would (on average) increase the trip time by 4.9 years and increasing K_t from 10 to 20% would only increase the trip time by one year. Furthermore, increasing the minimum r_{FB} from 5 to 10 Jupiter radii would increase the trip time by a range from 1.8 (Titan) to 3.5 (Med-Lite) years.

Numerical Results for NEP Spacecraft

The minimum-time transfers to the heliospheric boundary were obtained for the NEP spacecraft outlined earlier, and the results are presented in Table 7. Trajectories utilizing a chemically injected Earth escape and an NEP-powered spiral Earth escape are presented in this table. The initial circular Earth orbit for the spiral Earth escape is set at a nuclear safe altitude of 800 km (Ref. 3). All solutions employed a single Jupiter gravity assist, and a three-burn engine sequence was assumed for all cases.

The resulting NEP trajectories are much more direct than the SEP trajectories because NEP power is constant and the need to perform perihelion burns is eliminated. Therefore, the long aphelion coasting arcs are either removed altogether during the optimization process or replaced by short coasting arcs ($\Delta\theta \approx 30$ deg). These direct NEP trajectories typically involve near-continuous thrusting out to heliocentric distances ranging from 35 to 40 AU. As an example of these direct trajectories, the optimal heliocentric NEP trajectory for the Delta is presented in Fig. 5. As shown in Fig. 5, the spacecraft essentially spirals away from the sun and eventually achieves solar-system escape conditions just prior to the Jupiter flyby. The NEP-powered burn arc for this case is terminated at a distance of 36.3 AU (which is not shown in Fig. 5), at which point the spacecraft's speed is 12.5 AU/year.

As indicated in Table 7, an NEP trajectory could not be obtained for the Med-Lite because the smallest possible reactor and engine mass ($m_{pp} = 1230$ kg) is about 60% of the mass delivered by the Med-Lite to the nuclear safe circular Earth orbit. In addition, an NEP trajectory using a direct injection into heliocentric space via the upper stage of a Delta could not be obtained because the minimum m_{pp} is about 90% of the injected mass with $C_3 = 0$. The only possible NEP trajectory off a Delta must employ the NEP-powered Earth-escape spiral. The Earth-escape spiral lasts about 1.5 years for all three launch vehicles, and including the escape spiral reduces the trip time for the Atlas but increases the trip time for the Titan. The best NEP trajectories for the three launch vehicles exhibit better performance compared to the respective SEP cases with trip times ranging from 22.1 (Delta) to 18.2 (Titan) years. Although an NEP trajectory off a Titan can reach the heliospheric boundary in less than 20 years, the performance of an NEP spacecraft off a Delta is comparable and, therefore, probably preferable.

Table 7 Optimal trajectory and NEP parameters for minimum-time transfers with a Jupiter gravity assist

Launch vehicle	Launch date	Trip time, years	Escape time, years	C_3, km^2/s^2	P, kW	I_{sp}, s	ΔV_{GA}, km/s
Delta[a]	March 6, 2000	22.1	1.5	0.0	30.00	7000	18.8
Atlas	Oct. 1, 2001	25.8	0.0	0.63	30.00	7000	18.8
Atlas[a]	March 18, 2000	21.5	1.4	0.0	50.14	7000	15.6
Titan	Dec. 22, 2000	18.2	0.0	22.81	37.56	7000	18.7
Titan[a]	April 1, 2000	20.9	1.4	0.0	152.32	7000	16.0

[a]Utilizes Earth-escape spiral to $C_3 = 0$.

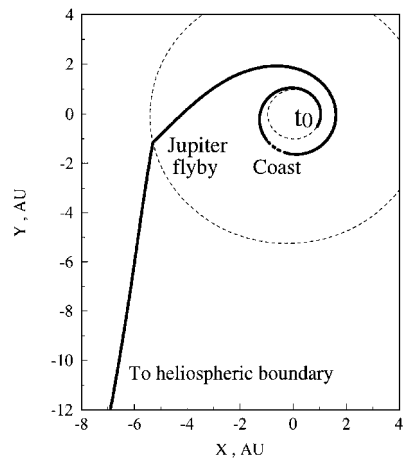

Fig. 5 Minimum-time NEP transfer: Delta with Jupiter gravity assist.

Conclusions

A new deep-space mission to the heliospheric boundary using ion propulsion spacecraft has been analyzed. The mission design is accomplished by solving a complex trajectory and propulsion system optimization problem. The goal is to minimize the total trip time to the heliospheric boundary; the design variables include launch date, launch energy, burn times, thrust vector direction, planetary flyby conditions, engine power, specific impulse, and arrival date.

Several optimal mission designs are obtained for spacecraft propelled by SEP and NEP for a wide range of launch vehicles. The best SEP trajectories exhibit total trip times ranging from 31.3 (Med-Lite launch vehicle) to 24.8 (Titan) years. The best NEP trajectories show trip times ranging from 22.1 (Delta) to 18.2 (Titan) years. The trip times for EP spacecraft are comparable or less than the trip times for spacecraft propelled by chemical systems. In particular, this analysis shows that SEP is capable of performing the mission off smaller launch vehicles (Med-Lite) in less time than an all-chemical system off larger launch vehicles (Delta). The NEP spacecraft show significant reductions in trip time compared to an all-chemical system for all launch vehicles. In addition, the overall mission analysis shows that the performance gap between large and small launch vehicles is narrowed by utilizing either SEP or NEP spacecraft. These results are perhaps surprising because EP has long been identified as an efficient means for performing space missions in terms of payload capabilities but not necessarily in terms of trip time savings. This analysis also demonstrates the advantages of using low-thrust spacecraft for high-energy deep-space missions.

Acknowledgments

This research was supported by the NASA Lewis Research Center under Grant NAG3-1731. The author would like to thank Mark Hickman for his suggestions and continual support during this project.

References

[1]Rayman, M. D., and Lehman, D. H., "NASA's First New Millennium Deep-Space Technology Validation Flight," International Academy of Astronautics, IAA Paper L-0502, April 1996.

[2]Meserole, J. S., and Richards, W. R., "Direct-Trajectory Options Using Solar Electric Propulsion for the Pluto Fast Flyby," IAA Paper 94-3253, June 1994.

[3]Vedder, J. D., Tabor, J. L., and Rusin, D. C., "Orbital Debris Hazard for Nuclear Electric Propulsion Earth-Escape Trajectories," *Journal of the Astronautical Sciences*, Vol. 41, No. 3, 1993, pp. 299–317.

[4]Gilland, J. H., "Mission and System Optimization of Nuclear Electric Propulsion Vehicles for Lunar and Mars Missions," NASA CR-189058, Dec. 1991.

[5]Gilland, J. H., and George, J. A., "Early Track NEP System Options for SEI Missions," AIAA Paper 92-3200, July 1992.

[6]Kluever, C. A., and Pierson, B. L., "Vehicle-and-Trajectory Optimization of Nuclear Electric Spacecraft for Lunar Missions," *Journal of Spacecraft and Rockets*, Vol. 32, No. 1, 1995, pp.126–132.

[7]Jones, R. M., "Comparison of Potential Electric Propulsion Systems for Orbit Transfer," *Journal of Spacecraft and Rockets*, Vol. 21, No. 1, 1984, pp. 88–95.

[8]Hermel, J., Meese, R. A., Rogers, W. P., Kushida, R. O., Beattie, J. R., and Hyman, J., "Modular, Ion-Propelled, Orbit-Transfer Vehicles," *Journal of Spacecraft and Rockets*, Vol. 25, No. 5, 1988, pp. 368–374.

[9]Mewaldt, R. A., Kangas, J., Kerridge, S. J., and Neugebauer, M., "A Small Interstellar Probe to the Heliospheric Boundary and Interstellar Space," *Acta Astronautica*, Vol. 35, Supplement, 1995, pp. 267–276.

[10]Oleson, S. R., "Influence of Power System Technology on Electric Propulsion Missions," AIAA Paper 94-4138, Aug. 1994.

[11] Oleson, S. R., "An Analytical Optimization of Electric Propulsion Orbit Transfer Vehicles," NASA CR-191129, May 1993.

[12] Fearn, D. G., "The Impact of Ion Propulsion on High Energy Interplanetary Missions," International Astronautical Federation, IAF Paper 94-U.4.487, Oct. 1994.

[13] Kluever, C. A., "Optimal Low-Thrust Interplanetary Trajectories by Direct Method Techniques," American Astronomical Society, AAS Paper 96-194, Feb. 1996.

[14] Pierson, B. L., "Sequential Quadratic Programming and Its Use in Optimal Control Model Comparisons," *Optimal Control Theory and Economic Analysis 3,* North-Holland, Amsterdam, 1988, pp. 175–193.

[15] Pouliot, M. R., "CONOPT2: A Rapidly Convergent Constrained Trajectory Optimization Program for TRAJEX," Convair Div., General Dynamics, GDC-SP-82-008, San Diego, CA, Jan. 1982.

[16] Sims, J. A., Staugler, A. J., and Longuski, J. M., "Trajectory Options to Pluto via Gravity Assists from Venus, Mars, and Jupiter," AIAA Paper 96-3614, July 1996.

[17] Perkins, F. M., "Flight Mechanics of Low-Thrust Spacecraft," *Journal of the Aerospace Sciences*, Vol. 26, No. 5, 1959, pp. 291–297.

J. A. Martin
Associate Editor